

## Letter

**Beta-gamma spectroscopy of the neutron-rich  $^{150}\text{Ba}$** 

R. Yokoyama<sup>1,\*</sup>, E. Ideguchi<sup>2,\*</sup>, G. S. Simpson<sup>3,\*</sup>, Mn. Tanaka<sup>2</sup>, S. Nishimura<sup>4</sup>, P. Doornenbal<sup>4</sup>, G. Lorusso<sup>4</sup>, P.-A. Söderström<sup>4</sup>, T. Sumikama<sup>5</sup>, J. Wu<sup>6</sup>, Z. Y. Xu<sup>7</sup>, N. Aoi<sup>2</sup>, H. Baba<sup>4</sup>, F. L. Bello Garrote<sup>8</sup>, G. Benzoni<sup>9</sup>, F. Browne<sup>4,10</sup>, R. Daido<sup>11</sup>, Y. Fang<sup>11</sup>, N. Fukuda<sup>4</sup>, A. Gottardo<sup>12,13</sup>, G. Gey<sup>3,14</sup>, S. Go<sup>1</sup>, N. Inabe<sup>4</sup>, T. Isobe<sup>4</sup>, D. Kameda<sup>4</sup>, K. Kobayashi<sup>15</sup>, M. Kobayashi<sup>1</sup>, I. Kojouharov<sup>16</sup>, T. Komatsubara<sup>17,18</sup>, T. Kubo<sup>4</sup>, N. Kurz<sup>16</sup>, I. Kuti<sup>19</sup>, Z. Li<sup>6</sup>, M. Matsushita<sup>1</sup>, S. Michimasa<sup>1</sup>, C. B. Moon<sup>20</sup>, H. Nishibata<sup>11</sup>, I. Nishizuka<sup>5</sup>, A. Odahara<sup>11</sup>, Z. Patel<sup>4,21</sup>, S. Rice<sup>4,21</sup>, E. Sahin<sup>8</sup>, H. Sakurai<sup>4,7</sup>, H. Schaffner<sup>16</sup>, L. Sinclair<sup>4,22</sup>, H. Suzuki<sup>4</sup>, H. Takeda<sup>4</sup>, J. Taprogge<sup>23,24</sup>, Zs. Vajta<sup>19</sup>, H. Watanabe<sup>4,25,26</sup>, A. Yagi<sup>11</sup> and T. Inakura<sup>27</sup>

<sup>1</sup>Center for Nuclear Study, the University of Tokyo, 2-1 Hirosawa, Wako, Saitama 351-0198, Japan

<sup>2</sup>Research Center for Nuclear Physics, Osaka University, 10-1 Mihogaoka, Ibaraki, Osaka 567-0047, Japan

<sup>3</sup>LPSC, 53 Rue des Martyrs, F-38026 Grenoble Cedex, France

<sup>4</sup>RIKEN Nishina Center, 2-1 Hirosawa, Wako-shi, Saitama 351-0198, Japan

<sup>5</sup>Department of Physics, Tohoku University, Aramaki-aza-aoba, Aoba, Sendai, Miyagi 980-8578, Japan

<sup>6</sup>School of Physics and State Key Laboratory of Nuclear Physics and Technology, Peking University, Beijing 100871, China

<sup>7</sup>Department of Physics, the University of Tokyo, 7-3-1 Hongo, Bunkyo-ku, Tokyo 113-8654, Japan

<sup>8</sup>Department of Physics, University of Oslo, P. O. Box 1072 Blindern, 0316 Oslo, Norway

<sup>9</sup>INFN, Sezione di Milano, I-20133 Milano, Italy

<sup>10</sup>School of Computing, Engineering and Mathematics, University of Brighton, Brighton BN2 4GJ, UK

<sup>11</sup>Department of Physics, Osaka University, Machikaneyama-chou 1-1, Osaka 560-0043 Toyonaka, Japan

<sup>12</sup>Dipartimento di Fisica dell'Università degli Studi di Padova, I-35131 Padova, Italy

<sup>13</sup>INFN, Laboratori Nazionali di Legnaro, Legnaro I-35020, Italy

<sup>14</sup>Institut Laue-Langevin, B.P. 156, F-38042 Grenoble Cedex 9, France

<sup>15</sup>Department of Physics, Rikkyo University, 3-34-1 Nishi-Ikebukuro, Toshima-ku, Tokyo 171-8501, Japan

<sup>16</sup>GSI Helmholtzzentrum für Schwerionenforschung GmbH, 64291 Darmstadt, Germany

<sup>17</sup>Research Facility Center for Pure and Applied Science, University of Tsukuba, Ibaraki 305-8577, Japan

<sup>18</sup>Rare Isotope Science Project, Institute for Basic Science, Daejeon 305-811, Korea

<sup>19</sup>MTA Atomki, P.O. Box 51, Debrecen, H-4001, Hungary

<sup>20</sup>Hoseo University, Asan, Chungnam 336-795, Korea

<sup>21</sup>Department of Physics, University of Surrey, Guildford GU2 7XH, UK

<sup>22</sup>Department of Physics, University of York, Heslington, York YO10 5DD, UK

<sup>23</sup>Instituto de Estructura de la Materia, CSIC, E-28006 Madrid, Spain

<sup>24</sup>Departamento de Física Teórica, Universidad Autónoma de Madrid

<sup>25</sup>International Research Center for Nuclei and Particles in the Cosmos, Beihang University, Beijing 100191, China

<sup>26</sup>School of Physics and Nuclear Energy Engineering, Beihang University, Beijing 100191, China

<sup>27</sup>Department of Physics, Niigata University, Niigata 950-2181, Japan

\*E-mail: yokoyama@cns.s.u-tokyo.ac.jp; ideguchi@rcnp.osaka-u.ac.jp; simpson@lpsc.in2p3.fr

Received December 23, 2017; Revised March 5, 2018; Accepted March 6, 2018; Published April 16, 2018

Excited states in the neutron-rich nucleus  $^{150}\text{Ba}$  have been observed via  $\beta$ - $\gamma$  spectroscopy at the Radioactive Isotope Beam Factory, RIKEN Nishina Center. The  $^{150}\text{Ba}$  ions were produced by the in-flight fission of a  $^{238}\text{U}$  beam with an energy of 345 MeV/nucleon. The  $E(2^+)$  energy of  $^{150}\text{Ba}$  was identified at 100 keV, which is the lowest known in the neutron-rich Ba isotopes. A  $\gamma$ -ray peak was also observed at 597 keV. A mean-field calculation with a fully 3D real space was performed and a static octupole deformation was obtained for the Ba isotopes.  $K^\pi = 0^-$  and  $1^-$  excited states with significant octupole collectivity were newly predicted at around or lower than 1 MeV on the ground state of  $^{150}\text{Ba}$  by a random-phase approximation calculation. The 597 keV  $\gamma$  ray can be interpreted as a negative-parity state, showing that  $^{150}\text{Ba}$  may possess octupole collectivity.

Subject Index D11, D12, D13, D29

One interesting feature of nuclear shell structure is that major shells in the  $l \cdot s$  coupling scheme contain high-spin, intruder orbits from the next oscillator shell. These orbits have the opposite parity to all others in the shell and are lowered in energy due to a strong spin-orbit interaction. Such intruder orbitals can cause higher-order interactions making, e.g., octupole-deformed shapes energetically favored in certain nuclei. Octupole correlations ( $\lambda = 3$ ) are caused by interactions between orbits with  $\Delta j = \Delta l = 3$  [1]. Nuclei with  $Z$  or  $N = 34, 56, 88$  and  $N = 134$  possess such orbits at or close to the Fermi surface and are expected to have strong octupole correlations [1]. There has been a long-standing question as to whether nuclei exist with a stable reflection asymmetric shape. Recently, static octupole deformation has been reported in the  $Z \sim 88, N \sim 134$  (Ra) region by Gaffney et al. [2] and around  $Z \sim 56, N \sim 88$  (Ba) by Bucher et al. [3]. In those works, large  $B(E3)$  values were measured directly by Coulomb excitation experiments.

The neutron-rich Ba isotopes from  $A = 140$  to 148 have been studied following the spontaneous fission of  $^{248}\text{Cm}$  and  $^{252}\text{Cf}$  [4–6] and negative-parity bands have been systematically observed up to intermediate spins. The enhanced  $E1$  transition rates of  $\gamma$  decays present between positive- and negative-parity bands are an indication of strong octupole correlations. However, Refs. [5,6] revealed that there is an unexpected trend in the  $E1$  rates of  $^{145,146}\text{Ba}$ , which are much slower than those of the neighboring  $^{144,148}\text{Ba}$ . The result that the  $E1$  rates in  $^{148}\text{Ba}$  were found to be as high as those of  $^{144}\text{Ba}$  raised a question as to whether more neutron-rich nuclei, such as  $^{150}\text{Ba}$ , also possess negative-parity states that are connected to a positive-parity band by strong  $E1$  decays. A microscopic-macroscopic calculation with a shell correction term, using a reflection asymmetric Woods-Saxon model, shows qualitative agreement with the experimental dipole moment obtained from the  $B(E1)/B(E2)$  rates [7]. In this calculation, the shell correction part explains the dip of the experimental dipole moment at  $^{146}\text{Ba}$  and all the even-even Ba isotopes from  $A = 144$  to 148 are predicted to possess static octupole deformation ( $\beta_3 \sim 0.075$  to 0.1). Quantitatively, however, the calculation for  $^{148}\text{Ba}$  underestimates the dipole moment and it is expected that there is a large uncertainty in the value predicted for  $^{150}\text{Ba}$ . Similarly, other theoretical works differ in their predictions of the size and extent of static octupole deformation in the neutron-rich Ba isotopes. Microscopic-macroscopic finite-range drop model calculations expect static octupole deformation to be present in  $^{141-147}\text{Ba}$  [8], whereas different covariant energy-density functionals predict this range to be  $^{144-150}\text{Ba}$ ,  $^{144-152}\text{Ba}$ , or  $^{146-148}\text{Ba}$  [9]. The generator-coordinate method (GCM) extension of the Hartree-Fock-Bogoliubov (HFB) calculation [10] predicts that the  $\beta_3$  value of  $^{150}\text{Ba}$  is as large as that of  $^{144-148}\text{Ba}$ .

Many negative-parity bands in the rare-earth region have been interpreted as octupole vibrations and the  $E(3^-)$  energy strongly depends on the amount of quadrupole deformation present [11]. In the rare-earth isotopes around  $Z \sim 60$ , a rapid onset of quadrupole deformation occurs when going from 88 to 90 neutrons. From the systematics of the  $E(2^+)$  energies or  $E(4^+)/E(2^+)$  ratios, the Ba isotopes also become quadrupole deformed as the neutron number increases. The onset of quadrupole deformation in the Ba isotopes is slower than that of  $Z \sim 60$  isotopes and the most neutron-rich Ba isotope measured to date,  $^{148}\text{Ba}$ , still has an  $E(4^+)/E(2^+)$  ratio smaller than 3.0.

It has become possible to access the neutron-rich  $A \sim 150$  Ba region at the Radioactive Isotope Beam Factory (RIBF) of the RIKEN Nishina Center. In-flight fission of a high-intensity  $^{238}\text{U}$  beam allows  $\beta$ - $\gamma$  and isomer spectroscopy studies of these neutron-rich nuclei.

Neutron-rich Ba ( $Z = 56$ ) isotopes were studied via  $\beta$ - $\gamma$  spectroscopy at RIBF. These nuclei were produced by the in-flight fission of a  $\sim 6$  pnA 345 MeV/nucleon  $^{238}\text{U}$  beam, which impinged on a 3 mm thick Be production target. Fission fragments were separated and identified in the BigRIPS in-flight separator [12] on an event-by-event basis by measurements of the mass-to-charge ratio ( $A/Q$ ) and atomic number ( $Z$ ). The  $A/Q$  value was obtained from time-of-flight (TOF) and magnetic rigidity ( $B\rho$ ) measurements in the second stage of BigRIPS. The TOF was measured by plastic scintillation detectors placed at two achromatic foci at the beginning (F3) and the end (F7) of the second stage of the BigRIPS beamline. The  $B\rho$  value was obtained by ion trajectory reconstruction using position and angular information measured by position-sensitive parallel-plate avalanche counters (PPACs) placed at the achromatic foci, F3, F7, and a dispersive focal plane, F5. The  $Z$  value was obtained by measuring the energy loss ( $\Delta E$ ) in an ionization chamber placed at the final F11 focal plane of the ZeroDegree spectrometer. A detailed explanation of the particle identification procedure at BigRIPS is found in Ref. [13]. During the  $\sim 50$  hours of beam time,  $2 \times 10^3$  ions of  $^{150}\text{Cs}$  were implanted in total.

The secondary beam was implanted into an active stopper, WAS3ABi [14]. This allowed energy and time information on a given implanted ion to be correlated with its subsequent detected  $\beta$  decay. The WAS3ABi detector consisted of five layers of double-sided-silicon-strip detectors (DSSSDs), each with  $40 \times 60$  strips. Each strip was 1 mm wide and each layer 1 mm thick. The  $x$  and  $y$  positions of the  $\beta$ -particle emission were obtained as the weighted mean position of the summed energy deposited in the neighboring strips, within a 200 ns time window. Since the dynamic range for the acquisition of the energy information of the Si strips was optimized for  $\beta$  particles, the  $x$ - $y$  positions of the ion-implantation point were obtained from the leading edge time of the analog signals from the DSSSDs. The events containing both detected ions and  $\beta$ -particle decays were defined as being correlated when their positions agreed to within a distance of 1 mm in the  $x$ - $y$  plane of the same Si layer. The time of each  $\beta$ -decay event was obtained from the difference in time-stamps between those recorded for ion implantation and  $\beta$ -particle detection. The maximum ion-implantation rate in WAS3ABi did not exceed  $\sim 30$  Hz, to preserve ion- $\beta$  correlations.

Any  $\gamma$  rays emitted after  $\beta$  decay were detected by EURICA [15,16], which is an array of EUROBALL cluster-type HPGe detectors [17], with 84 individual crystals in total. The total detection efficiency of the array for photons emitted from a point source at the center of the array with an energy of 1333 keV was  $\sim 8.4\%$ . The time window for  $\beta$ - $\gamma$  coincidences was 600 ns.

The  $\gamma$  rays detected following the  $\beta$  decay of  $^{150}\text{Cs}$  ions are shown in Fig. 1. Two peaks at 100 and 597 keV were assigned as transitions in  $^{150}\text{Ba}$ . The ion- $\beta$  time correlation window was limited to 200 ms, which was decided from the half-life of  $^{150}\text{Cs}$ , 0.84(8) ms. The  $\beta$ -decay half-lives measured in this experiment have already been published by Wu et al. [18].

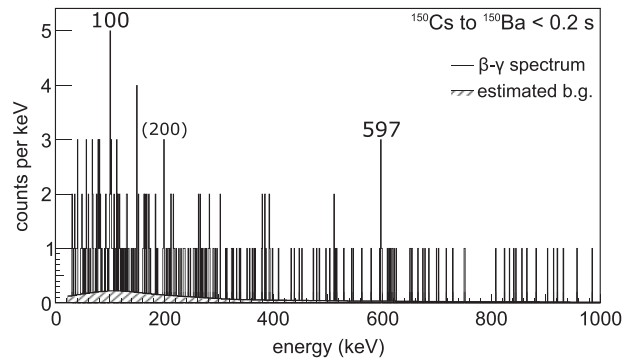


**Fig. 1.** A  $\gamma$ -ray spectrum from the  $\beta$  decay of  $^{150}\text{Cs}$ . Energies of the transitions correlated with the decay of  $^{150}\text{Cs}$  nuclei are labeled. The peak at 200 keV is identified as a  $\gamma$  ray following the decay of  $^{150}\text{Ba}$  (see text). The shaded area in the spectrum shows the level of the estimated continuum background, which is described in the text.

Since the number of peak counts was small, a log-likelihood ratio test was applied to the spectrum to see if the peaks are significant, compared to the continuum background. Here the test statistics,  $\sigma(E)$ , were defined as

$$\sigma(E) = \sqrt{B(E) + D(E)\ln(D(E)/B(E))}, \quad (1)$$

where  $D(E)$  is the number of counts at an energy,  $E$ , from the true event distribution, and  $B(E)$  is the number of estimated counts of continuum events at  $E$ . The continuum background was estimated by smoothing and scaling the energy spectrum with a time window of 2–10 s after ion implantation since this time region mainly consists of a constant component. The estimated curve of  $B(E)$  is shown by the shaded region in Fig. 1. The true event distribution,  $D(E)$ , was estimated to be the sum of the Gaussian distributions of all the events, which is

$$D(E) = \sum_{i=0}^{n_{\text{evt}}} \frac{1}{\sqrt{2\pi}\sigma_i} \exp\left(-\frac{(E - E_{\gamma i})^2}{2\sigma_i^2}\right), \quad (2)$$

where  $\sigma_i$  is the energy resolution of the Ge detector array and the energy  $E_{\gamma i}$  is the  $\gamma$ -ray energy of the  $i$ th event. Since our energy range of interest is roughly  $10^3$  times the energy resolution, a peak with the significance of  $3\sigma$  ( $\sim 0.3\%$ ) can reasonably appear *somewhere* in the spectrum. We requested a confidence level of more than  $4\sigma$  to define a significant peak in the spectrum of  $^{150}\text{Ba}$ .

Three peaks have maximum  $\sigma(E)$  values greater than  $4\sigma$ . These are situated at energies of 100, 200, and 597 keV and have  $\sigma$  values of 5.0, 4.4, and 4.3, respectively. The peak at 200 keV became more pronounced in a spectrum with a longer time window of up to 2 s after implantation, suggesting that this transition does not originate from an excited state of  $^{150}\text{Ba}$ . The peaks at 100 and 597 keV were assigned as  $\gamma$  rays from  $^{150}\text{Ba}$ , emitted following the  $\beta$  decay of  $^{150}\text{Cs}$ . There were no distinct peaks observed at 100 and 597 keV in a spectrum with a 2 s time window. The  $\beta$  decay from  $^{149}\text{Cs}$  to  $^{149}\text{Ba}$  was also studied and no peaks were found at these energies. However,  $^{149}\text{Ba}$  can also be produced by the  $\beta$ -delayed neutron decay of  $^{150}\text{Cs}$ .

The 100 keV  $\gamma$  ray was assigned as the decay of the first  $2^+$  state of  $^{150}\text{Ba}$ , from a comparison with the level energies of the neighboring Ba isotopes. The systematics of the excited states of Ba isotopes are shown in Fig. 2. The  $E(2^+)$  and  $E(4^+)$  systematics show an onset of quadrupole deformation at  $A \sim 144$ . We note that the first  $3^-$  state changes from the lowest negative-parity excitation to

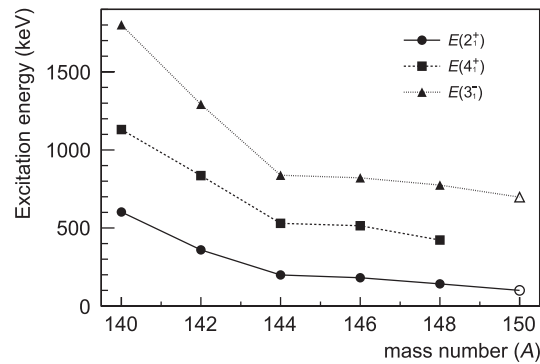


**Fig. 2.** Systematics of the excited states of even–even Ba isotopes. The lowest  $2^+$ ,  $4^+$ , and  $3^-$  states are shown. The  $(2^+)$  and  $(3^-)$  levels assigned tentatively in the present work are plotted in open symbols.

a member of the octupole vibrational band on a  $1^-$  state with the appearance of the quadrupole deformation. The systematic behavior of the low-lying negative-parity states with quadrupole deformation is discussed in Ref. [11]. The peak at 597 keV in  $^{150}\text{Ba}$  is a candidate for the  $\gamma$  decay of a negative-parity state. If the 597 keV  $\gamma$  ray is assigned tentatively as the  $3^- \rightarrow 2^+$  decay of  $^{150}\text{Ba}$ , then this fits with the systematics, as shown in Fig. 2. The assignment of the 597 keV peak as the  $1^- \rightarrow 0^+$  decay is less likely because of the fact that we do not observe an enhancement of the count at 497 keV, which is expected as the  $1^- \rightarrow 2^+$  decay. When the  $2^+$  state is a rotational excitation of the  $0^+$  ground state, the  $E1$  decay intensities from the  $1^-$  state to the  $0^+$  and  $2^+$  states should have similar strengths in Weisskopf units (W.u.) to each other. This means that we should see some counts at 497 keV, which are expected to be  $\sim 64\%$  of those at 597 keV by considering the  $\propto E^3 E1$  strength and the  $\gamma$  efficiency. The recent measurement at ISOLDE, CERN [19] is consistent with our assignments above. There are two possible events around 613 keV in our data where they report the  $1^- \rightarrow 0^+$  decay.

The global survey of Ref. [20] proposes the relation  $\beta_2 = (466 \pm 41)/AE(2_1^+)^{1/2}$ . For the neutron-rich  $A \sim 150$  region, there is a near-perfect agreement between  $\beta_2$  calculated using the above formula and the compilation of experimental data in Ref. [21] for the Ba–Sm isotopes. A value of  $\beta_2 = 0.31(3)$  for  $^{150}\text{Ba}$  can be extracted from  $E(2_1^+)$  measured in the present work. This is close to  $\beta_2 = 0.3588(36)$  measured for  $^{162}\text{Gd}_{92}$  [21], the highest one known in the region. Deformations of  $\beta_2 = 0.289, 0.237, 0.2585,$  and  $0.2792\text{--}0.2876$  have been predicted at  $^{150}\text{Ba}$  by four mean-field models, Hartree–Fock–Bogoliubov (HFB) [22], the finite-range droplet model (FRDM) [8], the universal energy-density functional (UNEDF1) [23], and GCM-HFB with the Gogny D1S interaction [10], respectively. Our result for the  $E(2_1^+)$  value possibly indicates a larger deformation than expected in  $^{150}\text{Ba}$ .

The spin and parity ( $J^\pi$ ) of the ground state of the parent nucleus,  $^{150}\text{Cs}$ , is not known. The most probable proton configuration of  $^{150}\text{Cs}$  is  $\pi 3/2^+$  [422] since this has been assigned as the ground state of  $^{143,145}\text{Cs}$  and was measured by an atomic beam magnetic resonance method [24]. The neutron configuration is not clear since  $J^\pi$  is not known for the ground states of any of the nearby  $N = 95$  isotones. The closest  $N = 95$  isotone with a firmly assigned ground state is  $^{159}\text{Gd}, \nu 3/2^-$  [521] [25], though the  $\nu 5/2^+$  [642] and  $\nu 5/2^-$  [523] quasiparticles lie  $< 150$  keV above this. However, the systematics of the experimental  $E(2^+)$  values indicates that Ba isotopes are less deformed compared to the Nd to Gd isotopes. We did not observe isomeric states in  $^{150}\text{Ba}$  in the time range  $\sim 300$  ns to a few tens of microseconds, in contrast to the  $N \geq 60$  rare-earth nuclei [26]. This indicates a change

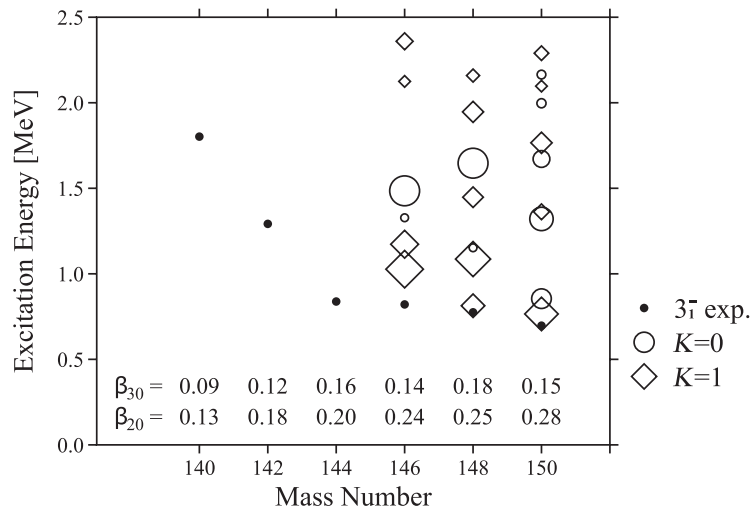


**Fig. 3.** Excitation energies of  $J^\pi = 3^-$  states obtained by an RPA calculation. The size of the symbols represents  $B(E3; 0^+ \rightarrow 3^-)$  of each state. Quadrupole and octupole deformation parameters ( $\beta_{30}$  and  $\beta_{20}$ ) of the ground states are shown in the plot.

in the structure of Ba isotopes compared to the rare-earth isotopes and is not clear enough to tell the ground state of  $^{150}\text{Cs}$ .

Following the Gallagher–Moszkowski coupling rules, the possible ground-state spins of  $^{150}\text{Cs}$  are  $(0^-)$ ,  $(1^+)$ , and  $(4^-)$ , respectively. The configurations of states in  $^{150}\text{Ba}$  likely to be populated following allowed  $\beta$  decays of  $^{150}\text{Cs}$  can be estimated using the procedures outlined in Ref. [27]. Transitions are allowed between states obeying the selection rules of  $\Delta N = 0$ ,  $\Delta n_z + \Delta \Lambda = 0$ ,  $|\Delta n_z| = 2$ ,  $\Delta K = 0, 1$ . The  $\nu 3/2^- [521]$  and  $\nu 5/2^- [523]$  orbitals can decay to the  $\pi 3/2^- [541]$  and  $\pi 5/2^- [532]$  ones via allowed transitions. A  $(\pi 3/2^+ [422] \otimes \pi 3/2^- [521])_{0^-}$   $^{150}\text{Cs}$  ground state would populate either  $(\pi 3/2^+ [422] \otimes \pi 3/2^- [541])_{0^-}$  or  $(\pi 3/2^+ [422] \otimes \pi 5/2^- [532])_{1^-}$  2-quasiparticle states. We note also that in this region first-forbidden transitions are predicted to compete with allowed ones accounting for  $\sim 60\%$  of the decay intensity [28]. This may explain the low statistics observed in Fig. 1 as first-forbidden transitions can fragment the feeding and also directly populate the  $^{150}\text{Ba}$  ground state. For a  $J^\pi = (4^-)$  ground-state assignment of  $^{150}\text{Cs}$ ,  $\beta$  decay can reasonably feed a  $J^\pi = 3^-$  member of the bands with strong  $(\pi 3/2^+ [422] \otimes \pi 3/2^- [541])_{0^-}$  or  $(\pi 3/2^+ [422] \otimes \pi 5/2^- [532])_{1^-}$  configurations. This does not, however, firmly establish the  $J^\pi$  of the ground state of  $^{150}\text{Cs}$  because other excited states can be populated, which then decay via unobserved higher-energy  $\gamma$  rays.

A theoretical calculation of the neutron-rich Ba isotopes was performed in order to compare the excitation energies of the  $J^\pi = 3^-$  states with the experimental ones. The static properties were obtained by a Hartree–Fock calculation and the random-phase approximation (RPA) was applied to it in a self-consistent manner in order to calculate the properties of excited states [29,30]. In this calculation, a fully 3D real-space representation, without any spatial symmetry, was used in order to allow shape-breaking spatial symmetries, such as octupole deformed shapes, to be included. The SkM\* force [31] was employed, though pairing correlations were not taken into account.

Static octupole deformations ( $\beta_{30} = 0.093$  to  $0.177$ , shown in Fig. 3) appear in the ground states of the  $N = 84$  to  $94$  Ba isotopes. There is a local minimum in the octupole moments at  $A = 146$ , which is consistent with the systematics of the experimental dipole moments in Ref. [6]. The gradual

increase of the quadrupole deformation ( $\beta_2$ ), when heading towards the neutron-rich isotopes, is also consistent with the systematics of the experimental  $E(2^+)$  values shown in Fig. 2. The calculation predicts that  $^{150}\text{Ba}$  also has a ground-state octupole deformation as large as those of the even–even  $A = 144$  to  $148$  isotopes.

The results of the RPA calculation on the Ba isotopes are shown in Fig. 3. Excitation energies of  $J^\pi = 3^-$  states were calculated for  $^{146,148,150}\text{Ba}$ , along with  $K = 0^-$  and  $1^-$  excitations, which are predicted at energies of  $\sim 1$  MeV or lower. The lowest  $J = 3$  excitation of  $^{150}\text{Ba}$ , at 0.76 MeV, has  $B(E3) = 35$  W.u., which indicates that the octupole excitation is a collective state rather than a single-particle one. Our calculation suggests that there can be a negative-parity state with octupole collectivity as low as  $\sim 700$  keV.

In summary,  $\beta$ – $\gamma$  spectroscopy on the most neutron-rich Ba isotope measured to date,  $^{150}\text{Ba}$ , was performed. The  $E(2^+)$  energy of  $^{150}\text{Ba}$  was determined to be 100 keV, which indicates that the quadrupole deformation of  $^{150}\text{Ba}$  increases compared to that of  $^{148}\text{Ba}$ . Although the peak at 597 keV cannot be definitely assigned, the interpretation of this  $\gamma$  ray as the decay from a negative-parity  $J = 3$  state does not contradict the present experimental or theoretical results. An HF-plus-RPA calculation was performed in a fully self-consistent manner for the neutron-rich Ba isotopes. The calculation predicted a static octupole deformation in the  $A = 140$  to  $150$  Ba isotopes and  $K = 0$  and  $1$  excitations with octupole collectivity at around, or less than, 1 MeV in  $^{146-150}\text{Ba}$ . The RPA calculation supports the existence of a negative-parity state in  $^{150}\text{Ba}$ , a candidate for which was obtained in this work at an energy of 697 keV. The result appears to show that  $^{150}\text{Ba}$  has large octupole collectivity and that the region of octupole correlations around  $Z = 56$ ,  $N = 88$  may be wider than expected.

## Acknowledgements

We acknowledge financial support from KAKENHI (25247045). This work was carried out at the RIBF operated by RIKEN Nishina Center, RIKEN, and CNS, the University of Tokyo. We acknowledge the EUROBALL Owners Committee for the loan of germanium detectors and the PreSpec Collaboration for the readout electronics of the cluster detectors. Part of the WAS3ABi was supported by the Rare Isotope Science Project, which is funded by the Ministry of Science, ICT and Future Planning (MSIP) and National Research Foundation (NRF) of Korea. This work was supported by the Spanish Ministerio de Ciencia e Innovación under Contract Nos. FPA2009-13377-C02 and FPA2011-29854-C04 and the Hungarian Research Fund (OTKA), Contract No. K100835. R.Y. was supported by the ALPS program of the University of Tokyo and by a JSPS fellowship No. JP15J10788.

## References

- [1] I. Ahmad and P. A. Butler, *Ann. Rev. Nucl. Part. Sci.* **43**, 71 (1993).
- [2] L. P. Gaffney et al., *Nature* **497**, 199 (2013).
- [3] B. Bucher et al., *Phys. Rev. Lett.* **116**, 112503 (2016).
- [4] W. R. Phillips, I. Ahmad, H. Emling, R. Holzmann, R. V. F. Janssens, T.-L. Khoo, and M. W. Drigert, *Phys. Rev. Lett.* **57**, 3257 (1986).
- [5] S. J. Zhu et al., *Phys. Lett. B* **357**, 273 (1995).
- [6] W. Urban et al., *Nucl. Phys. A* **613**, 107 (1997).
- [7] P. A. Butler and W. Nazarewicz, *Nucl. Phys. A* **533**, 249 (1991).
- [8] P. Möller, A. J. Sierk, T. Ichikawa, and H. Sagawa, *At. Data Nucl. Data Tables* **109–110**, 1 (2016).
- [9] S. E. Agbemava, A. V. Afanasjev, and P. Ring, *Phys. Rev. C* **93**, 044304 (2016).
- [10] L. M. Robledo and G. F. Bertsch, *Phys. Rev. C* **84**, 054302 (2011).
- [11] P. D. Cottle and D. A. Bromley, *Phys. Lett. B* **182**, 129 (1986).
- [12] T. Kubo, *Nucl. Instrum. Meth. Phys. Res. B* **204**, 97 (2003).
- [13] T. Ohnishi et al., *J. Phys. Soc. Japan* **79**, 073201 (2010).

- [14] S. Nishimura, Prog. Theor. Exp. Phys. **2012**, 03C006 (2012).
- [15] S. Nishimura et al., RIKEN Accelerator Progress Report **46**, 182 (2013). Available at: [http://www.nishina.riken.jp/researcher/APR/index\\_e.html](http://www.nishina.riken.jp/researcher/APR/index_e.html).
- [16] P.-A. Söderström et al., Nucl. Instrum. Meth. Phys. Res. B **317**, 649 (2013).
- [17] J. Eberth et al., Prog. Part. Nucl. Phys. **28**, 495 (1992).
- [18] J. Wu et al., Phys. Rev. Lett. **118**, 072701 (2017).
- [19] R. Lică et al. [IDS Collaboration], Phys. Rev. C **97**, 024305 (2018).
- [20] S. Raman, C. W. Nester, and P. Tikkanen, At. Data Nucl. Data Tables **78**, 1 (2001).
- [21] B. Pritychenko, M. Birch, B. Singh, and M. Horoi, At. Data Nucl. Data Tables **107**, 1 (2016).
- [22] J.-P. Delaroche, M. Girod, J. Libert, H. Goutte, S. Hilaire, S. Péru, N. Pillet, and G. F. Bertsch, Phys. Rev. C **81**, 014303 (2010).
- [23] M. Kortelainen, J. McDonnell, W. Nazarewicz, P.-G. Reinhard, J. Sarich, N. Schunck, M. V. Stoitsov, and S. M. Wild, Phys. Rev. C **85**, 024304 (2012).
- [24] C. Ekström, L. Robertsson, G. Wannberg, and J. Heinemeier, Phys. Scr. **292**, 144 (1977).
- [25] A. Y. Cabezas, I. Lindgren, and R. Marrus, Phys. Rev. **122**, 1796 (1961).
- [26] G. S. Simpson, W. Urban, J. Genevey, R. Orlandi, J. A. Pinston, A. Scherillo, A. G. Smith, J. F. Smith, I. Ahmad, and J. P. Greene, Phys. Rev. C **80**, 024304 (2009).
- [27] P. C. Sood and R. K. Sheline, At. Data Nucl. Data Tables **43**, 259 (1989).
- [28] T. Marketin, L. Huther, and G. Martínez-Pinedo, Phys. Rev. C **93**, 025805 (2016).
- [29] T. Nakatsukasa, T. Inakura, and K. Yabana, Phys. Rev. C **76**, 024318 (2007) [[arXiv:nucl-th/0703100](https://arxiv.org/abs/nucl-th/0703100)] [[Search INSPIRE](#)].
- [30] T. Inakura, T. Nakatsukasa, and K. Yabana, Phys. Rev. C **80**, 044301 (2009) [[arXiv:0906.5239](https://arxiv.org/abs/0906.5239) [nucl-th]] [[Search INSPIRE](#)].
- [31] J. Bartel, P. Quentin, M. Brack, C. Guet, and H.-B. Håkansson, Nucl. Phys. A **386**, 79 (1982).